



# Estimating groundwater recharge using deep vadose zone data under typical irrigated cropland in the piedmont region of the North China Plain



Leilei Min<sup>a</sup>, Yanjun Shen<sup>a,\*</sup>, Hongwei Pei<sup>a,b</sup>

<sup>a</sup> Key Laboratory of Agricultural Water Resources, Center for Agricultural Resources Research, Institute of Genetics and Developmental Biology, Chinese Academy of Sciences, Shijiazhuang 050021, PR China

<sup>b</sup> University of the Chinese Academy of Sciences, 19A, Yuquan Road, Beijing 100049, PR China

## ARTICLE INFO

### Article history:

Received 16 January 2015

Received in revised form 17 April 2015

Accepted 27 April 2015

Available online 6 May 2015

This manuscript was handled by Corrado Corradini, Editor-in-Chief, with the assistance of Xunhong Chen, Associate Editor

### Keywords:

Groundwater recharge process

Deep vadose zone

North China Plain

## SUMMARY

Groundwater recharge can be accurately estimated by understanding the soil water flow process in the deep vadose zone. In this study, soil water content and soil matric potential were measured in situ in the deep vadose zone (~8 m) under typical irrigated cropland in the piedmont region of the North China Plain and were used to analyze the soil water dynamics and calibrate a transient matric flow model. Using the calibrated model, the long-period average groundwater recharge was estimated, and the influences of the lower boundary depth and time scale (length of study period) on the recharge were assessed. The study showed that the response time of the water table (with a buried depth of 42 m) to water input might be no more than 1 year because the velocity of the wetting front could be as high as 0.13 m/day below the root zone. However, the lag time could be more than 15 years because of the slower velocity of the soil water displacement. The variation in the recharge flux with depth was significant over shorter time scales. Therefore, for more representative estimated recharge with a maximum deviation less than 20% from the 38-year mean value, research should be conducted over a long period (>12 years). However, the average annual recharge showed almost no change with depth at the 38-year scale, and a depth of 2 m below ground surface could be used as an interface for estimating recharge at the 38-year scale. The simulated annual recharge at a depth of 2 m ranged from 59 mm to 635 mm with a mean value of 200 mm. The variation in water input (precipitation and irrigation) was the main reason for the variation in annual recharge at the depth of 2 m. This approach improves our understanding of the recharge process in the deep vadose zone in this region, and the results of this work could aid development of effective groundwater resources management.

© 2015 Elsevier B.V. All rights reserved.

## 1. Introduction

Groundwater recharge is of fundamental importance in evaluating groundwater resources and meeting agricultural water requirements. In an area with a deep water table, downward soil water flux from the bottom of the root zone (deep drainage) is often referred as potential recharge (Rushton, 1988; de Vries and Simmers, 2002; Radford et al., 2009; Wohling et al., 2012). Generally, if deep drainage is not hampered by low-conductivity horizons in the deep vadose zone or flow to nearby local depressions (where it runs off or evaporates), it could eventually completely recharge the groundwater with a delay (de Vries and Simmers, 2002). However, soil water flux in deep vadose zone

usually varies with depth and time because of variations in water input (precipitation and irrigation) pulses, variations in evapotranspiration, and changes in deep soil water storage (Hubbell et al., 2004; West and Truss, 2006; Timms et al., 2012). Therefore, the deep vadose zone plays an important role in groundwater recharge process. The soil water dynamics and soil water flux in deep vadose zone have attracted much attention (Hubbell et al., 2004; Rimón et al., 2007; Dahan et al., 2009; Kurtzman and Scanlon, 2011; Turkeltaub et al., 2014), but further studies are necessary to better understand the process of groundwater recharge.

The piedmont area of the North China Plain is a high-yield agricultural area with widely distributed farmland (Shen et al., 2002; Sun et al., 2010). Grain production in this area is maintained by groundwater over-exploitation (Yuan and Shen, 2013). As a result, the excessive exploitation of groundwater resources has caused a continuous decline in the water table. Vertical recharge caused

\* Corresponding author. Tel./fax: +86 311 85825464.

E-mail address: [yjshen@sjziam.ac.cn](mailto:yjshen@sjziam.ac.cn) (Y. Shen).

by precipitation and irrigation is the dominant recharge mechanism in the piedmont area (von Rohden et al., 2010), which is also the key hydrological process that connects precipitation, irrigation and groundwater. Therefore, estimation of vertical groundwater recharge is a prerequisite for sustainable development of groundwater resources.

In recent years, unsaturated zone methods (physical methods, tracer methods and numerical modeling) for estimating groundwater recharge have been fully tested and broadly applied. In the piedmont area of the North China Plain, these methods have been used to estimate the groundwater recharge in irrigated areas (Xue and Gao, 1987; Qiu, 1992a; Kendy et al., 2003; Wang et al., 2008; Lu et al., 2011; Ma et al., 2011; Lin et al., 2013; Tan et al., 2014). Based on these studies, the potential groundwater recharge rates over short time scales (a short-term length of the study period, i.e., one to several years) at fixed low boundary depths (~2 m) are generally well understood. However, the recharge process in the deep vadose zone (variation in flux with depth, velocity of the wetting front, etc.) is less understood. Most of these studies only used datasets from shallow depths or sparse sediment samples of the deep vadose zone, and as a result, the dynamic process of groundwater recharge in the deep vadose zone could not be revealed. In addition, the mean value of multi-year recharge could not be accurately estimated from these studies since the findings in different studies might display considerable differences given that these works were conducted at different time scales (with different water inputs) and at variable low boundary depths. The modeling method is useful for estimating groundwater recharge. However, research that used both water content data and matric pressure data (rather than soil water content only) for model calibration is limited, which leads to less credible parameters and induces uncertainty into the results (Šimůnek and Hopmans, 2002). Using the dataset from the deep vadose zone combined with a numerical model, both the dynamic nature of the soil water flow (velocity of the wetting front, variation in flux with depth, etc.) and the effects of water input, time scales and depth of lower boundary on the recharge could be elucidated.

The objective of this study was to investigate the groundwater recharge process in the deep vadose zone (~8 m) under typical irrigated cropland in the piedmont region of the North China Plain. To achieve this objective, in situ monitoring data, chloride mass balance (CMB), soil water budget, and numerical simulation were used to: (i) interpret the characteristics of the soil water dynamics and evaluate the response time of the water table to water input, (ii) calibrate the transient unsaturated flow and estimate the long-period average groundwater recharge using the calibrated model, and (iii) assess the impact of the lower boundary depth and time scale on the soil water flux.

## 2. Materials and methods

### 2.1. Experimental sites and instrumentation setup

The experiments were conducted at the Luancheng Experimental Station for Agro-ecosystems at the Chinese Academy of Sciences (37°53'N, 114°41'E, altitude of 50.1 m), which is located in the middle of the piedmont area in the North China Plain (Fig. 1a), with a semi-arid to semi-humid monsoonal climate. The mean annual precipitation is 496 mm (1971–2013), most of which occurs from July to September, and the mean annual temperature at the station is 13.2 °C (1971–2013). A one-year double cropping agro-system, i.e., winter wheat and summer maize, is predominantly adopted in this region. Generally, 3–5 irrigation applications of ~80 mm each are carried out in the winter wheat growing season, and 0–2 irrigation applications of ~80 mm each

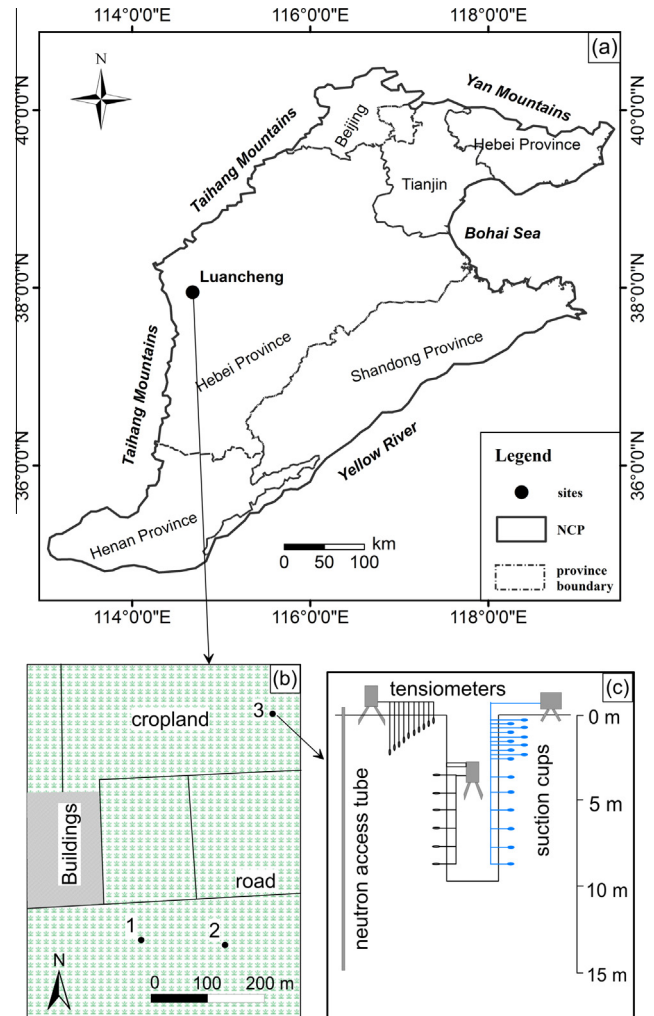


**Fig. 1.** Location of the experimental site in the North China Plain (a), observation positions at the site (b), and schematic of soil profile instrumentation (c). Points 1, 2 and 3 in (b) are the locations of the monitoring well, eddy covariance system, and deep vadose zone monitoring systems, respectively.

are carried out in the summer maize growing season (Zhang et al., 2003, 2011; Sun et al., 2010). The water table depth has increased dramatically from 11 m in 1975 to 42 m in 2013 at a drawdown rate of approximately 0.84 m per year.

The ET was measured (Fig. 1b) by an eddy covariance system composed of a CSAT3 sonic-anemometer (Campbell Scientific, Inc.) and a LI7500 H<sub>2</sub>O/CO<sub>2</sub> gas analyzer (Li-Cor, Inc.) installed at a height of 3 m above the ground surface. The latent heat flux was measured every 30 min. A deep vadose zone monitoring system was established based on an old open caisson (constructed in the 1970s with an inner diameter of 150 cm and a depth of 900 cm) in which the inner sidewall was brick lined (Fig. 1c). Soil water content and matric potential in the deep vadose zone were measured, and the soil solution was sampled. A borehole constructed with a 15.2-m deep aluminum access tube was used to measure soil water content through a neutron probe (IH-II, Institute of Hydrology, Wallingford, UK) at 10-cm intervals from a depth of 0 to 100 cm and at 20-cm intervals from a depth of 100 to 1500 cm. The matric potential was measured by tensiometers at 20-cm intervals from a depth of 0 to 200 cm and at 100-cm intervals from a depth of 200 to 800 cm. The porous ceramic cup of the tensiometer was placed at a location approximately 1 m from the sidewall (Fig. 1c). Both soil water content and matric potential

were measured with a time interval of no more than 10 days. The dataset for ET, soil water content and matric potential over a period from 1 December 2011 to 30 September 2013 was used in this study.

Rainfall, irrigation water and soil pore water sampling campaigns were conducted during a two-year period (2011–2013). Rainfall was collected immediately after each rainfall event, and irrigation water was collected when cropland was irrigated. Soil pore water was collected by a vacuum extraction system. The anion Cl amount was measured via an ion chromatography system (ICS-2100) at the Center for Agricultural Resources Research, Institute of Genetics and Developmental Biology at the Chinese Academy of Sciences.

## 2.2. Chloride mass balance (CMB) method

The CMB method (Eq. (1)) (Scanlon et al., 2010) was used to estimate the average annual recharge rate. By assuming (1) the sources of chloride are rainfall and irrigated water, (2) there is no contribution of chloride from weathering, (3) the surface runoff is negligible, and (4) the soil water movement is one-dimensional downward and vertical, the chloride input from precipitation ( $P$ ) and irrigation ( $I$ ) balances the chloride output in recharge ( $R$ ),

$$R = (PC_p + IC_I) / C_{sm} \quad (1)$$

where  $C_p$  and  $C_I$  are the average chloride concentration in the rainfall and irrigation water, respectively, and  $C_{sm}$  is the depth-weighted average chloride concentration in the soil pore water in the deep vadose zone (below 2 m).

## 2.3. Soil water budget

Assuming that the surface runoff is negligible, the soil water budget equation (Eq. (2)) in a vertical soil column is expressed as follows:

$$D = P + I - ET_a - \Delta S \quad (2)$$

where  $D$  is the drainage out of the bottom of the column;  $P$ ,  $I$  and  $ET_a$  are precipitation, irrigation and actual evapotranspiration, respectively; and  $\Delta S$  is the change in water storage in the column.

## 2.4. Transient matrix flow modeling in the vadose zone

The HYDRUS-1D model was used to simulate the transient matrix flow. The HYDRUS-1D model is a one-dimensional physically based model that can be used to simulate soil water flow and solute transport (Šimůnek et al., 2013). The soil hydraulic

parameters in the model were calibrated by the dataset from 1 October 2011 to 30 September 2012 and validated by the dataset from 1 October 2012 to 30 September 2013, respectively. The calibrated model was used to simulate the soil water flux from 1 January 1976 to 31 December 2013.

### 2.4.1. Governing equation

The mathematical model used in the HYDRUS-1D model is described as follows:

$$\frac{\partial \theta}{\partial t} = \frac{\partial}{\partial z} \left[ K(h) \left( \frac{\partial h}{\partial z} + 1 \right) \right] - S(h) \quad (3)$$

where  $\theta$  is the volumetric water content,  $t$  is time,  $K$  is the unsaturated hydraulic conductivity,  $h$  is matric potential,  $z$  is the vertical coordinate (assumed to be 0 at the ground surface and increased downward), and  $S$  is the root water uptake.

The van Genuchten–Mualem relationships were used (Mualem, 1976; van Genuchten, 1980) to model the soil hydraulic properties as follows:

$$\theta(h) = \begin{cases} \theta_r + \frac{\theta_s - \theta_r}{(1 + |\alpha h|)^{1-1/n}} & h < 0 \\ \theta_s & h \geq 0 \end{cases} \quad (4)$$

$$K(h) = K_s \left( \frac{\theta - \theta_r}{\theta_s - \theta_r} \right)^l \left\{ 1 - \left[ 1 - \left( \frac{\theta - \theta_r}{\theta_s - \theta_r} \right)^{n/(n-1)} \right]^{1-1/n} \right\}^2 \quad (5)$$

where  $\theta_r$  is the residual volumetric water content,  $\theta_s$  is the saturated volumetric water content,  $\alpha$  is the air entry parameter,  $n$  is the pore size distribution parameter,  $l$  is the pore connectivity parameter and  $K_s$  is the hydraulic conductivity. Except the pore connectivity parameter ( $l$ ), which was set to be 0.5 according to Jimenez-Martinez et al. (2009), the other parameters in Eqs. (4) and (5) were calibrated and validated.

### 2.4.2. Initial and boundary conditions

The initial condition is described as

$$h(z, 0) = h_0(z) \quad (6)$$

When the model was calibrated and validated, the flux boundary condition was selected as the upper boundary condition, as described in Eq. (7):

$$\frac{\partial h}{\partial z} \Big|_{z=0} = \frac{P + I - E}{k(h)} - 1 \quad (7)$$

where  $P$  is precipitation,  $I$  is irrigation and  $E$  is actual evaporation. Actual evaporation and transpiration were separated from the measured evapotranspiration by the measured leaf area index (Šimůnek et al., 2013) (see Fig. 2).

When the calibrated model was used to simulate the soil water flux from 1 January 1976 to 31 December 2013, the upper boundary condition was set as the atmospheric condition, which was implemented as follows. Firstly, the reference crop evapotranspiration  $ET_0$  was calculated using the FAO-PM equation (Allen et al., 1998). Secondly, the crop potential evapotranspiration  $ET_c$  was calculated by multiplying  $ET_0$  with a crop coefficient. Thirdly, the potential evaporation ( $E_c$ ) and crop potential transpiration ( $T_c$ ) were separated by Beer's Law and the leaf area index (Šimůnek et al., 2013).

The free drainage type boundary condition described in Eq. (8) is used to simulate the lower boundary of the model because the groundwater table (42 m below ground surface) is far below the lower boundary of the model (8 m below ground surface) (Šimůnek et al., 2013).

$$\frac{\partial h}{\partial z} (L, t) = 0 \quad (8)$$

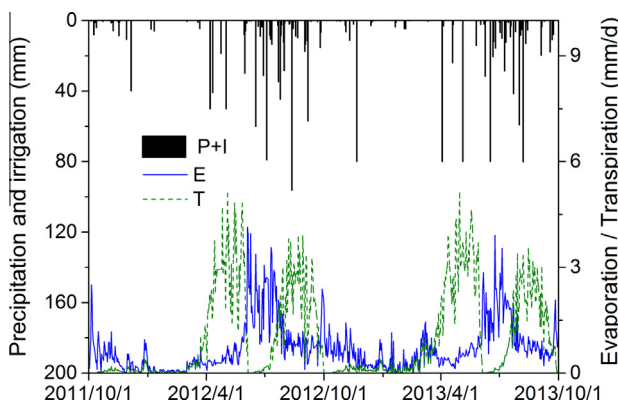


Fig. 2. Water input ( $P$  and  $I$ ), actual evaporation ( $E$ ) and transpiration ( $T$ ) during the monitoring period of 1 October 2011–30 September 2013.

### 2.4.3. Root water uptake

The root water uptake was calculated based on the Feddes-type uptake functions (Feddes et al., 1978).

$$S(h) = \lambda(x)\alpha(h)T_p \quad (9)$$

where  $\lambda(x)$  is the relative root distribution function,  $\alpha(h)$  is a dimensionless water stress response function, and  $T_p$  is the potential transpiration rate estimated from the potential evapotranspiration and leaf area index.

The relative root distribution  $\lambda(x)$  was described in the following function according to the user's manual of the HYDRUS-1D model (Šimůnek et al., 2013):

$$\lambda(x) = \begin{cases} \frac{1.667}{L_r} & x > L - 0.2L_r \\ \frac{2.0833}{L_r} \left(1 - \frac{L-x}{L_r}\right) & x \in (L - L_r; L - 0.2L_r) \\ 0 & x < L - L_r \end{cases} \quad (10)$$

where  $L$  is the  $x$ -coordinate of the ground surface, and  $L_r$  is the root depth. It should be noted that the bottom of the soil profile is located at  $x=0$  and the ground surface at  $x=L$  in Eq. (10). The growth of the roots was adopted from Liu and Wang (1999) and Zhang et al. (2004).

The dimensionless water stress  $\alpha(h)$  displays a relationship with the soil water matric potential (Feddes et al., 1978). During the course of model calibration and validation, the potential transpiration in Eq. (9) was replaced by actual transpiration, and the dimensionless water stress  $\alpha(h)$  were set to 1, ensuring the optimal root water uptake. When the calibrated model was applied to assess the multi-year (1976–2013) groundwater recharge, the default parameter values of the matric potential of wheat and maize based on Wesseling et al. (1991) were used to simulate the root water uptake.

### 2.4.4. Spatial and temporal discretization

The modeled soil column ranged from the ground surface to a depth of 8 m, the same maximum depth at which soil water content and matric potential were measured. The modeled soil column was vertically discretized with a spacing of 2 cm. A self-adjusting numerical time stepping scheme, with minimum and maximum time step of 0.0001 days and 5 days, respectively, was used during the simulations. The relative fine spatial discretization and the self-adjusting numerical time stepping scheme could ensure the numerical convergence and water balance during simulations in this study.

### 2.4.5. Goodness-of-fit assessment

The soil column was divided into 13 layers, and the van Genuchten–Mualem model parameters of each layer were calibrated and validated (Table 1). To reduce the parameter uncertainty, both soil water content and matric potential, rather than soil water content only, were used to calibrate the model. The root mean square error (RMSE) and mean absolute error (MAE) were selected as the criteria for quantifying the deviation of the modeled results from the observed data.

$$RMSE = \sqrt{\frac{1}{n} \sum_{i=1}^n (P_i - O_i)^2} \quad (11)$$

$$MAE = \frac{1}{n} \sum_{i=1}^n |P_i - O_i| \quad (12)$$

where  $n$  is the number of observations, and  $P_i$  and  $O_i$  are the simulated and observed values of the  $i$ th observation, respectively.

**Table 1**

The calibrated van Genuchten–Mualem hydraulic parameters for different soil layers.

Depth (cm)	Soil texture	$\theta_r$ (cm <sup>3</sup> /cm <sup>3</sup> )	$\theta_s$ (cm <sup>3</sup> /cm <sup>3</sup> )	$\alpha$ (1/cm)	$n$ (-)	$K_s$ (cm/day)
0–60	Silt loam	0.07	0.42	0.03	1.45	100.30
60–100	Silt loam	0.09	0.41	0.04	1.30	30.50
100–120	Silt clay loam	0.08	0.33	0.01	1.16	17.00
120–190	Silt loam	0.10	0.40	0.03	1.25	25.40
190–220	Silt loam	0.10	0.44	0.03	1.15	22.90
220–270	Silt loam	0.12	0.36	0.01	1.18	98.70
270–360	Silt loam	0.09	0.41	0.01	1.30	49.86
360–420	Silt loam	0.09	0.40	0.01	1.40	69.84
420–480	Silt loam	0.10	0.42	0.02	1.28	61.01
480–570	Loamy sand	0.05	0.40	0.03	1.45	129.04
570–720	Sand	0.05	0.30	0.06	2.02	598.50
720–780	Silt loam	0.08	0.38	0.04	2.11	142.50
780–800	Sandy loam	0.10	0.40	0.03	1.35	35.50

### 2.5. Evaluation of variation in groundwater recharge with time scales

It is necessary to analyze the effect of the length of study period on the error in recharge estimation (Jiménez-Martínez et al., 2010). To investigate the influence of time scales on the annual recharge rate, we introduced an index ( $\varepsilon_{\max}^{(k)}$ ), which is the maximum bias of the soil water flux ( $D_{ij}^{(k)}$ ) at a certain depth over different time scales ( $k$ ) deviated from the 38-year mean annual recharge. The annual recharge from 1976 to 2013 (represented by  $i$ , from 1 to 38) were simulated by the transient matrix flow modeling at the depth of 2–8 m (represented by  $j$ , from 2 to 8) at 1-m intervals. The matrix  $\{D_{ij}\}$  ( $i = 1, 2, \dots, 38; j = 2, 3, \dots, 8$ ) was used to contains the annual recharge at different depths. Then, at a certain depth  $j$ , the matrix  $\{D_{ij}\}$  was averaged over different time scales ( $k = 1, 2, \dots, 30$ ) using the smoothed moving average method, creating 30 matrices, i.e.,  $\{D_{ij}^{(k)}\}$  ( $i = 1, 2, \dots, 38; j = 2, 3, \dots, 8; k = 1, 2, \dots, 30$ ). Finally, the values of  $\varepsilon_{\max}^{(k)}$  at a certain depth were evaluated using Eq. (13):

$$\begin{cases} \varepsilon_1^{(k)} = \frac{\max\{D_{ij}^{(k)}\} - \bar{D}}{\bar{D}} \\ \varepsilon_2^{(k)} = \frac{\bar{D} - \min\{D_{ij}^{(k)}\}}{\bar{D}} \\ \varepsilon_{\max}^{(k)} = \max\{\varepsilon_1^{(k)}, \varepsilon_2^{(k)}\} \end{cases} \quad (13)$$

where  $\bar{D}$  is the 38-year mean annual recharge,  $D_{ij}^{(k)}$  is  $k$ -year (the middle of the periods is the  $i$ th or  $i+1$ th year) mean annual recharge at the depth of  $j$ ,  $\varepsilon_1^{(k)}$  and  $\varepsilon_2^{(k)}$  is the bias of the soil water flux at time scale  $k$  deviated from the 38-year mean annual recharge, respectively.

## 3. Results

### 3.1. Velocity of the wetting front and response time of the recharge to water input

The profiles of soil water content and total soil water potential in both wet and dry periods were illustrated in Fig. 3. In the root zone (0–2 m), soil moisture varied dramatically due to precipitation, irrigation, root water uptake and evaporation. Beneath the root zone, soil water content changed slightly, by no more than 0.05 in volumetric content. The variation in total soil water potential (in this study, total potential equals to the sum of matric potential and gravitational potential with reference level at ground surface) demonstrated that the direction of the soil water flux within the root zone (0–2 m) could be directed upward and

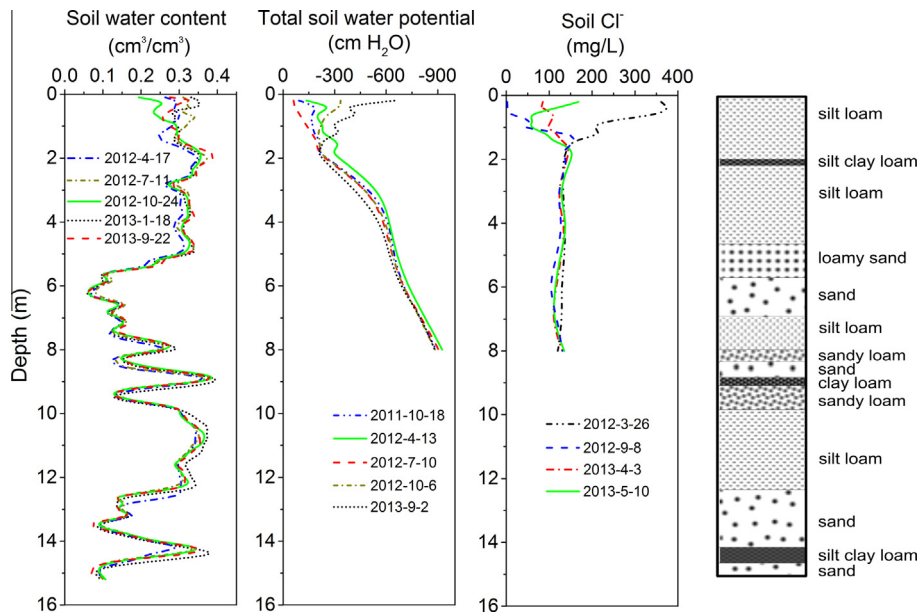


Fig. 3. Variations in soil water content, total soil water potential, and chloride concentration with depth.

downward (Fig. 3). The maximum depth of the zero flux plane could be located as deep as 2 m because of evaporation and root water uptake, which implied that the soil water in the root zone (0–2 m) escaped via evapotranspiration and deep drainage. At the depth of 2–5 m, total soil water potential still exhibited considerable variation, implying that an unsteady downward soil water flux existed in this zone. At the depths deeper than 5 m, the variation in total water potential was the smallest (Fig. 3). Therefore, from the perspective of vadose zone modeling, the lower boundary condition could be assumed to be unit gradient at a layer deeper than 5 m.

The temporal variation in soil water content and soil water pressure head at a typical depth was plotted in Fig. 4. As mentioned previously, soil water content and pressure head showed greater variation when the soil layer is closer to the land surface. According to the monitored matric potential and water content, responses to intensive rain events and irrigation could be observed even at a depth of 8 m within two months (Fig. 4). The mean propagation velocity of the wetting front could be estimated by investigating the response time at different depths. The estimated mean propagation velocity of the wetting front in the 2–8 m soil layers ranged from 0.12 to 0.14 m/day. The small discrepancy may be caused by soil spatial heterogeneity because the water content measurement and pressure head measurement were not collected exactly at the same location. In the piedmont region in the North China Plain, Qiu (1992b) found that the velocity of the wetting front after water input is approximately 0.15 m/day. Rimón et al. (2007) discovered that the mean propagation velocity of the wetting front in the sandy loam and sand soil layers is approximately 0.2 m/day. The mean propagation velocity of the wetting front obtained in this study was consistent with the above mentioned research.

The response time ( $t_1$ ) was used to refer to the time during which the water table requires a response to deep drainage pulse, and can be estimated by Eq. (14):

$$t_1 = \frac{L}{v_w} \quad (14)$$

where  $L$  is the depth from the bottom of root zone (2 m) to the water table (42 m), and  $v_w$  is the velocity of the wetting front. As mentioned previously, the estimated propagation velocity of the

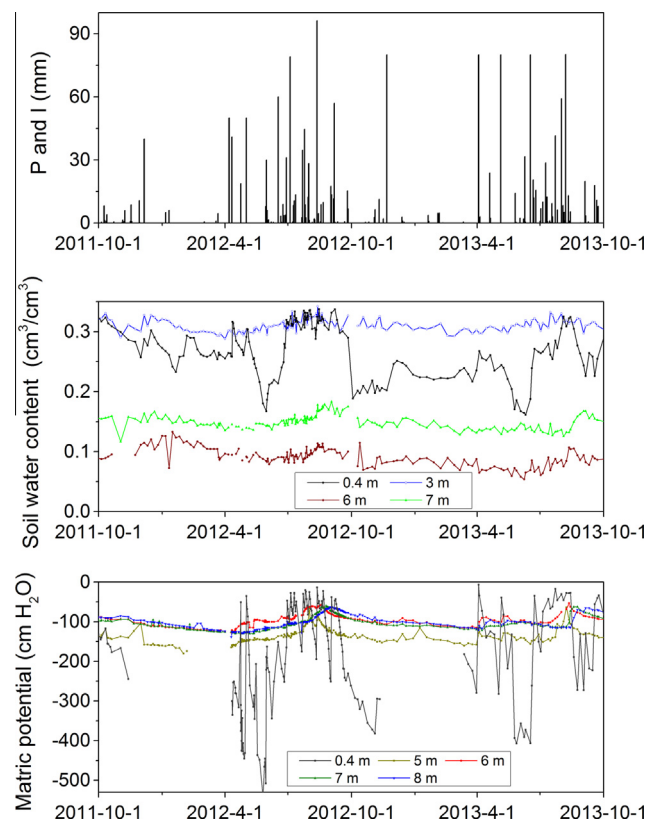


Fig. 4. Temporal variations in water content and matric potential at typical soil depths.

wetting front in the 2–8 m soil layers was about 0.13 m/day in average. Assuming that no impeding water layer existed between 8 m and the water table (42 m) and that the hydrogeological condition did not differ between the 2–8 m layers and 8–42 m layers, the response of the water table (42 m) to potential recharge would be no more than 1 year. In fact, from the published reports, the soil textures in the 8–42 m layers are silt loam, silt lacy loam sandy

loam and sand (Zhang and Fei, 2009; He et al., 2013), which means that the difference in lithology between the 2–8 m layer and the 8–42 m layers was not obvious. Lu et al. (2011) reported that the response time would be 1 month (the depth to water table is approximately 35 m) based on numerical modeling in this study area. The difference in soil layers configuration and soil texture-related parameters in the numerical model between this study and that of Lu et al. (2011) might be the reason for the disparity.

### 3.2. Calibration and validation of the transient matrix flow model

The measured and simulated water content and matric potential at four typical layers were plotted in Fig. 5. The simulated soil water contents in the four typical layers agreed well with the measured values. During the calibration process, the average RMSE and MAE values were near 0.017 and 0.015, respectively, while during the validation process, the average RMSE and MAE values were approximately 0.03 and 0.022. As shown in Fig. 5, the simulated soil water matric potential could also capture the change in the measured soil water matric potential. It is necessary to note that there was a delay in the arrival time of modeled wetting front compared to that of the measurement in deep vadose zone (Fig. 5). In this study, soil water content and matric potential were emphasized for the parameter calibration. If the arrival time of the wetting front was also considered, as investigated by Turkeltaub et al. (2015), the delay of the wetting front between modeled and measured results may be reduced, while the importance of soil water content and matric potential in inverse solution would be impaired. Besides, preferential flow may be one of the reasons that lead to the delay of arrival time of modeled wetting front.

The simulated and measured soil water storages in the 0–800 cm profile were shown in Fig. 6. The number of dots below the 1:1 line was more than that of the dots above, which implied that modeled soil water storage values were slightly less than the measured ones. However, the coefficient of correlation ( $R^2$ )

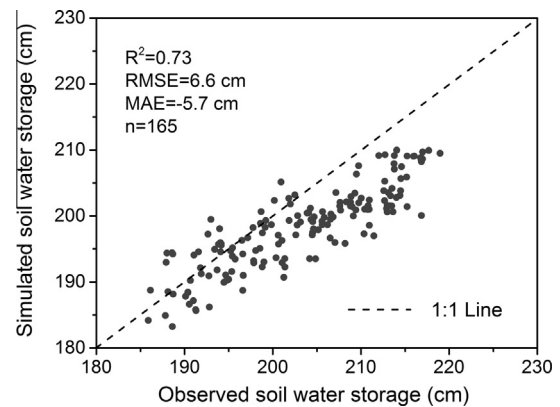


Fig. 6. Comparison between the simulated and measured soil water storage in the profile from 0 to 800 cm.

was 0.73, and the RMSE and MAE were 6.6 cm and  $-5.7$  cm, respectively, which indicated that the change in field soil water storage could be mostly modeled.

The groundwater recharge rate was also used to validate the model. During the period from 1 October 2011 to 30 September 2013, the amounts for precipitation and irrigation were 1095 mm and 591 mm, respectively. During the same period, the evapotranspiration measured by the eddy covariance systems was 1252 mm, and the change in soil water storage in the 0–8 m soil column was  $-21$  mm. Hence, the deep drainage at the 8-m depth was 455 mm based on Eq. (2). The simulated deep drainage during this period was approximately 440 mm. The deep drainage obtained from the numerical simulation matched well with that obtained from Eq. (2), which indicated that the calibrated model simulated the soil water flux successfully. Therefore, the calibrated model was subsequently used to evaluate the field water cycle under different water input conditions.

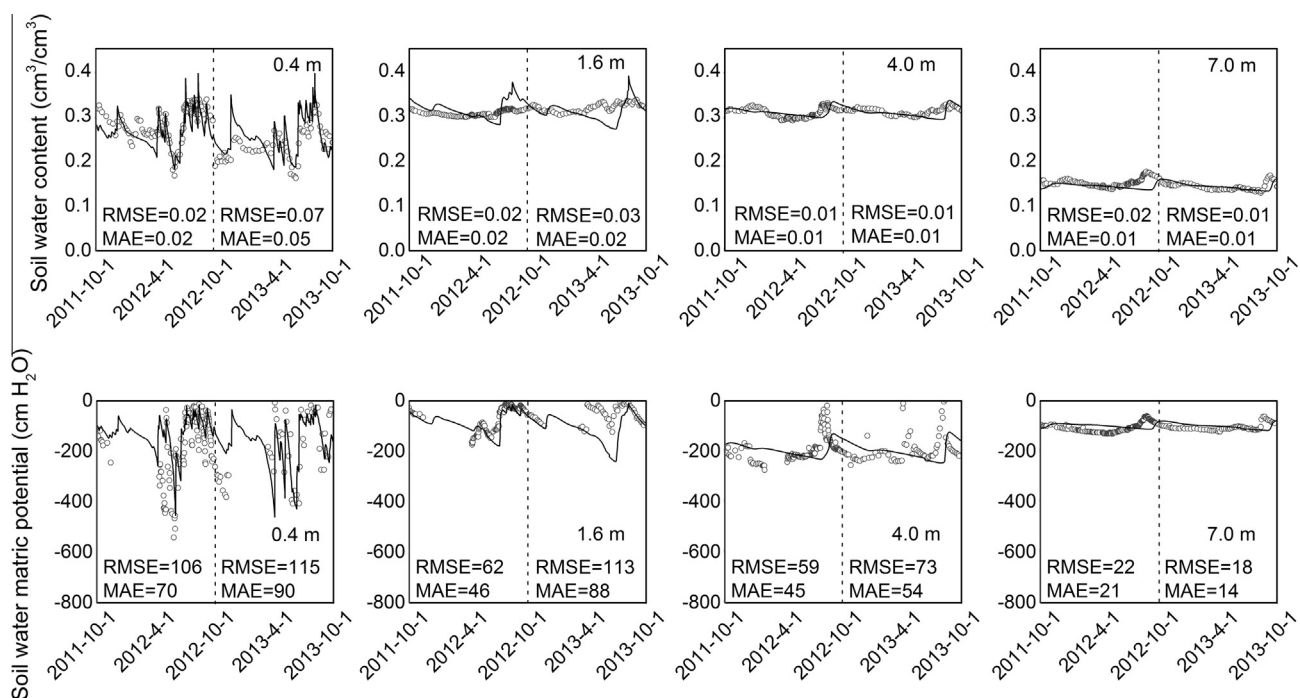


Fig. 5. Comparison between the simulated (line) and measured (circles) water content and simulated matric potential at typical soil depths.

### 3.3. Estimation of the mean annual groundwater recharge using the numerical model and CMB approach

#### 3.3.1. Recharge estimation using numerical modeling

To investigate the influence of water input on the groundwater recharge, the groundwater recharge from 1971 to 2013 was modeled. The results from 1976 to 2013 were used for analysis because the first five years were used for model equilibrium due to a lack of initial conditions.

The actual irrigation time and annual irrigation amounts during the past 38 years were absent. However, the irrigation time and irrigation amount could be estimated according to Zhang et al. (2003) and Sun et al. (2010). The farmers' irrigation schedule involved irrigating crops at four key periods for winter wheat (pre-dormancy, revival jointing, heading and filling) and two key periods for maize (seeding and jointing), with ~80 mm of water applied in each irrigation event. Therefore, the irrigation schedule used in this study approximated the actual irrigation schedule as follows: if the precipitation was less than the precipitation at 75% probability, the six key periods listed above must be irrigated, but if the precipitation was greater than the precipitation at 25% probability, only four key periods for winter wheat were irrigated; otherwise, the four key periods for winter wheat and the seeding period for maize were irrigated.

The annual recharge rates from 1976 to 2013 at a depth of 2 m as estimated by the model ranged from 59 mm to 635 mm with a mean value of 200 mm (Fig. 7). Tan et al. (2014) found that most areas of the predominant plain experience the values of recharge rates approximately 166–234 mm/year from 2001 to 2009, according to the INFIL 3.0 model. Focusing on the Luancheng Station in the piedmont plain, the recharge rate is 51–245 mm/year (from August in 2003 to September in 2005) based on the Br-tracer experiment (Wang et al., 2008) and 180 mm/year in 2004 based on the HYDRUS-1D model (Lu et al., 2011). Kendy et al. (2004) reported that the annual recharge ranges from 50 mm to 1090 mm during the period from 1949 to 2000 at the Luancheng County. It is clear that these previous results are consistent with the results from this study. According to the modeled results, the net groundwater consumption for typical cropland was approximately 200 mm/year (irrigation minus vertical recharge), which was close to the difference between precipitation and evapotranspiration determined by the micrometeorological method (Shen et al., 2013). Because vertical recharge is the main recharge mechanism in this study area, the groundwater recharge is less than the groundwater extraction for irrigation. The accumulated net consumption of groundwater by agriculture could well explain the change of water table depth (Fig. 8).

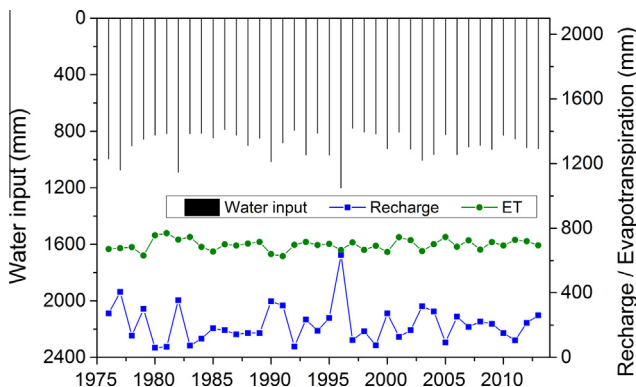


Fig. 7. Long-term simulated annual groundwater recharge compared with the annual water input and actual evapotranspiration at the depth of 2 m during the period from 1976 to 2013.

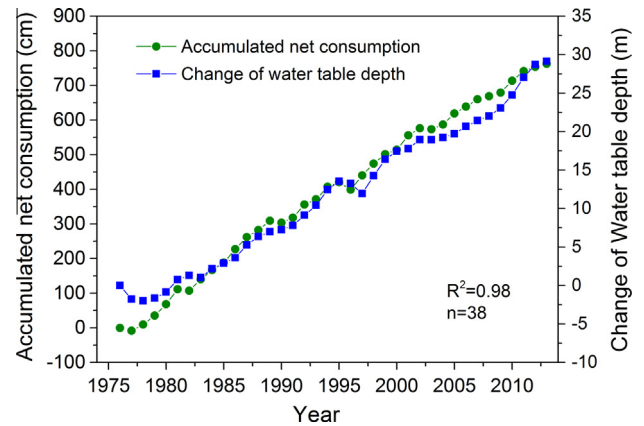


Fig. 8. High correlation of the simulated accumulated net groundwater consumption (annual irrigation minus recharge) and observed change in the water table depth.

#### 3.3.2. Recharge estimation based on the CMB approach

The chloride concentration of precipitation, irrigated water and soil pore water were 7.0 mg/l, 42.5 mg/l and 125 mg/l, respectively (Fig. 3). The total irrigation amount was approximately 400 mm/year in the past decades. The annual mean precipitation was approximately 496 mm/year. Therefore, the multi-year average groundwater recharge calculated by the CMB method was approximately 164 mm/year.

The 38-year mean recharge rate (200 mm/year) from numerical modeling differed from the recharge rate estimated by the CMB method (164 mm/year). This inconformity was not surprising due to the differences in the data type and quantity and the different simplifications of reality in both models (Kurtzman and Scanlon, 2011). In addition, the percolating water in deep vadose zone may not reach full chemical equilibrium with the total solute potential and the solute in vadose zone may not be totally flushed and displaced (Amiaz et al., 2011; Rimón et al., 2011). Therefore, when the CMB method was used, the pore-scale preferential flow would also lead to the under-estimation of groundwater recharge.

In this study, the recharge rates from the numerical model were believed to be more accurate and closer to the real situation because the numerical model included more mechanisms and fewer simplifications than the CMB method. Thus, the recharge rates estimated by the numerical model at different depths were used for further analysis.

### 3.4. Variation in groundwater recharge with depth and time scales

The groundwater recharge rate at different soil depths could be estimated by applying the soil water budget. Fig. 9a displayed the variation of soil water flux with depth. During the period from 1 October 2011 to 30 September 2012, the soil water flux reached a nearly steady rate (with a value of approximately 250 mm/year) from depths of 2 m to 7 m. The flux decreased from ~250 mm/year at a depth of 7 m to ~160 mm/year at a depth of 15 m. However, during the period from 1 October 2012 to 30 September 2013, the soil water flux increased with increasing depth, from ~190 mm/year at a depth of 2 m to ~300 mm/year at a depth of 15 m. If the calculated period was longer, from 1 October 2011 to 30 September 2013, the variation of soil water flux with depth was smaller. The simulated soil water flux at different depths in typical years is shown in Fig. 9b. It can be seen that the soil water flux showed significant variation with depth at these typical years. However, the 38-year average soil water flux was nearly steady (200 mm/year) below a depth of 2 m. The simulated and calculated

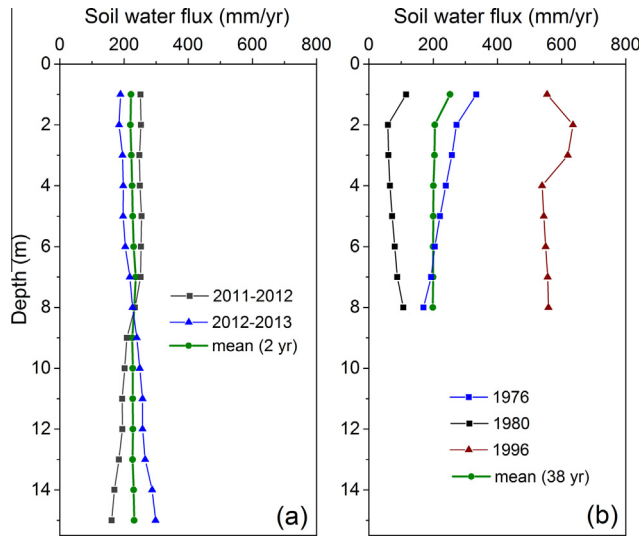


Fig. 9. Variations in the recharge flux with soil depth; (a) calculated values based on soil water budget; (b) simulated values using numerical model.

soil water flux values at different depths demonstrated that the soil water flux is both time and depth dependent. The temporal change of the groundwater recharge was primarily caused by different water input and climate factors, which have been reported by some research (Kendy et al., 2004; Leterme and Mallants, 2012; Wang et al., 2008). However, the variation in potential groundwater recharge with depth and time scale has not received sufficient attention. In this study, Fig. 10 showed that the maximum bias at different depths could be reduced at longer time scales. Moreover, when the soil water flux at a certain depth was used to represent the 38-year average potential recharge, the maximum bias could exceed 20% if the time scale (length of study period) was less than 13 years (Fig. 10).

Not only the total amount of recharge but also the recharge process varied at different depths. During the rainy season (from July to September), the recharge flux began to response to water input. Not surprisingly, the response of the soil water flux to a water input event at the 8-m depth was slower than that of the 2-m depth, with a lag time of approximately 50 days (Fig. 11). The peak flux at the 2-m depth could exceed 15 mm/day in the rainy season, whereas the peak flux at the 8-m depth was only approximately 2 mm/day. Therefore, these results clearly illustrate that the effect of the water input pulse was dampened with increased depth,

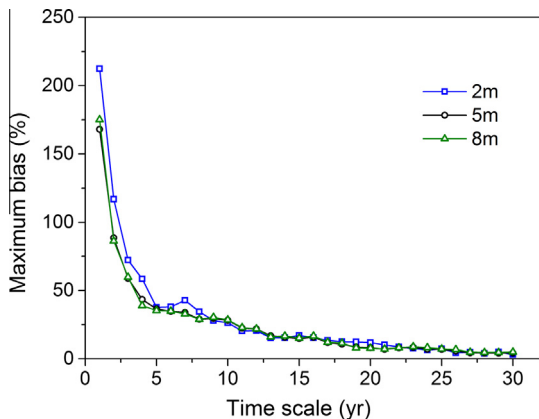


Fig. 10. Influence of time scales on the maximum deviation of the average annual recharge rate from the 38-year average annual recharge.

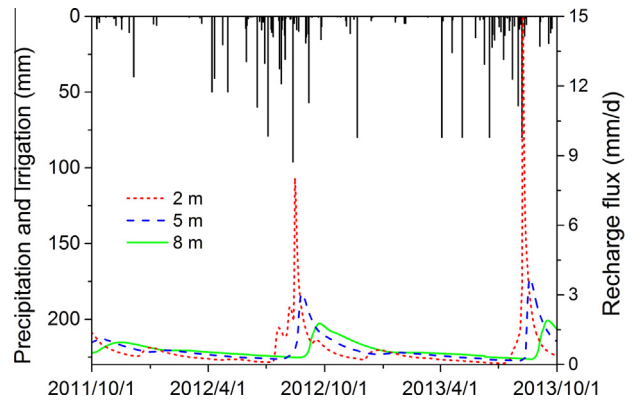


Fig. 11. Daily recharge flux at typical soil depths. The response of flux to water input was delayed, and the peak flux was dampened with increased depth.

resulting in a smaller peak flux in the deeper soil layer but a longer duration (Fig. 11). This result captured the important characteristics of soil water flux in the soil column at different depth in the deep vadose zone (Carrera-Hernandez et al., 2012). In brief, these results imply that the estimated groundwater recharge rate may have considerable bias from the multi-year average recharge if the calculated period was too short and the effect of depth was not considered.

### 3.5. Influence of water input on groundwater recharge

The recharge rate had a significant linear relationship with the water input ( $n = 38, p = 0.000, R^2 = 0.79$ ), and the water input could explain 79% of the total variance in the annual recharge rate (Fig. 12). The ratio of recharge to water input (recharge coefficient) is an important and helpful coefficient for hydrogeologists to

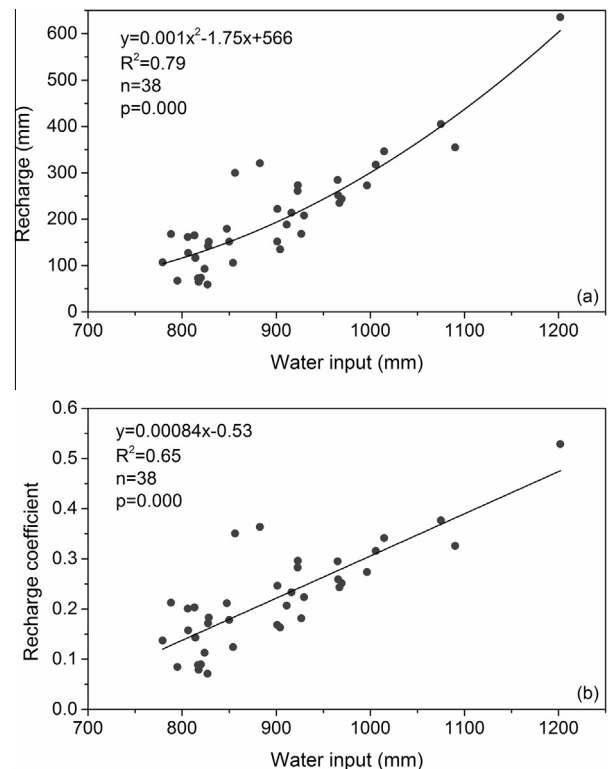


Fig. 12. Effect of water input on the recharge flux (a) and recharge coefficient (b) at the depth of 2 m.

quickly estimate the groundwater recharge. During this period, as shown in Fig. 12, the recharge coefficient varied from 0.07 to 0.53. The mean value of the recharge coefficient was approximately 0.22. Other studies reported that the recharge coefficient during the period from 1999 to 2005 at the Luancheng Station has a wide range, from 0.13 to 0.31 (Kendy et al., 2003; Lu et al., 2011; Wang et al., 2008). The large range of this value in this study may result from the variation of water input and dynamic soil water content. It is important to note that the irrigation input in the model was not exactly the actual irrigation amount applied by farmers because of lack of irrigation monitoring, and hence, the estimated recharge rate and recharge coefficient based on the model might exhibit a little difference from the actual recharge coefficient.

## 4. Discussion

### 4.1. Relationship among recharge flux, velocity of the wetting front and velocity of the soil water displacement

Water movement in the soil mostly follows the rule of piston flow, namely, the new water pushes out and displaces the old water (Zimmermann et al., 1966). The velocity of the soil water displacement (new water pushing old water) is an important indicator for evaluating groundwater pollution.

The recharge flux ( $q$ ) can be estimated using the velocity of soil water displacement ( $v_s$ ) and the average volumetric water content ( $\bar{\theta}$ ) via the Eq. (15) (Scanlon et al., 2007):

$$q = \bar{\theta} \cdot v_s \quad (15)$$

During the periods of the wetting front propagated from the 2-m depth to the 8-m depth, approximately from the first days in July to the first days in September (Fig. 4), the recharge flux could be estimated using Eq. (16) (Dahan et al., 2009; Rimón et al., 2007) based on the velocity of the soil water ( $v_w$ ) and the average change in the volumetric water content ( $\Delta\bar{\theta}$ ) in the 2–8 m layers.

$$q = \Delta\bar{\theta} \cdot v_w \quad (16)$$

Therefore, based on the piston flow hypothesis, the relationship between the velocity of the soil water wetting front ( $v_w$ ) and the velocity of the soil water displacement ( $v_s$ ) can be described by Eq. (17), which is the same as the equation deduced by Scanlon et al. (2007).

$$\frac{v_w}{v_s} = \frac{\bar{\theta}}{\Delta\bar{\theta}} \quad (17)$$

In this study, during the periods of the wetting front propagate from the 2-m depth to the 8-m depth, the average volumetric water content ( $\bar{\theta}$ ) was approximately 0.244, and the average change of the volumetric water content ( $\Delta\bar{\theta}$ ) was approximately 0.012 in the 2–8 m soil layers (Fig. 3), which led to the observation that the value of  $v_w$  (0.13 m/day) might be 20 times greater than the value of  $v_s$  (2.34 m/year) calculated by Eq. (17).

During the period from 1 October 2011 to 30 September 2013, the  $v_s$  obtained from Eq. (15) was approximately 0.92 m/year based on the average volumetric water content ( $\bar{\theta}$ ) of 0.24 and the recharge flux of 0.22 m/year. In comparison, the  $v_s$  calculated from Eq. (17) (2.34 m/year, during the periods of the propagation of the wetting front) is greater than that obtained from Eq. (15) (0.92 m/year, mean annual value). The result implies that the soil water displacement is a non-uniform and transient process.

In the piedmont plain, Qiu (1992a) estimated that the velocity of the soil water displacement ranges from 0.22 m/year to 0.7 m/year, and Tan et al. (2014) reported that the value ranges

from 0.2 m/year to 0.67 m/year. Both studies were conducted within the 0–8 m soil layers. However, using environmental tracers, Chen et al. (2006) and von Rohden et al. (2010) estimated that the displacement velocity of new water pushing old water ( $v_s$ ) is 2–2.6 m/year when the studied depths are both greater than 20 m. The discrepancy may indicate that the displacement velocity of new water pushing old water in the deeper soil layers (>8 m) is faster than that of the 0–8 m layers and that the deeper soil layers (>8 m) has a greater water transport capacity.

The lag time ( $t_2$ ) represents the delay during which water and solute are pushed from a certain depth to the water table in a 'piston flow' manner. In this study, the lag time equals to the depth from the bottom of the root zone to the water table ( $L$ ) divided by the velocity of the soil water displacement ( $v_s$ ), as described in Eq. (18) (Scanlon et al., 2007).

$$t_2 = \frac{L}{v_s} \quad (18)$$

Certainly, the response time ( $t_1$ ) is not the lag time ( $t_2$ ). Because the downward propagation of pressure wave transfers from the top layers to the deep layers greatly exceed velocity of the solute front, the deep soil water content will quickly respond to water input, and the velocity of the wetting front would be greater than the velocity of soil water displacement, resulting in a shorter response time than the lag time. If the results reported by Chen et al. (2006) and von Rohden et al. (2010) are used, the difference between the response time (~1 year) and lag time (15.4–20 years) is obvious.

In this study, the depths of the soil layers monitored for investigating the velocity of soil water wetting front ( $v_w$ ) and the displacement velocity of new water pushing old water ( $v_s$ ) was limited to 8 m. This result suggested that the deeper vadose zone should be investigated in future for more accurate estimation of the response time and lag time.

### 4.2. Uncertainty in the groundwater recharge rate estimation

Uncertainty is inevitable in estimating groundwater recharge because the actual recharge rates are unknown (Healy and Scanlon, 2010). An incorrect conceptual model, uncertainty in the parameters of the numerical model, and measurement errors in the hydrological variables could contribute to uncertainty in estimating the recharge rates (Healy and Scanlon, 2010).

It has been broadly recognized that preferential flow could exist in cropland soil (Beven and Germann, 2013; Harter et al., 2005; Hillel, 1998; Kurtzman and Scanlon, 2011), including the piedmont region of the North China Plain (Wu, 2013). In this study, preferential flow was not considered in the conceptual models (the numerical model and the CMB method), which may increase the uncertainties in the estimated groundwater recharge. Furthermore, the hysteresis effect was not included in the conceptual model, which rendered the conceptual model a simplification of reality, and hence, the model contains certain limitations (Carrera-Hernandez et al., 2012).

Model parameter uncertainty could be investigated via a simple sensitivity analysis (Jimenez-Martinez et al., 2009; Lu et al., 2011). In this study, the sensitivity analysis is implemented using the methods as presented in Jimenez-Martinez et al. (2009) and Lu et al. (2011), i.e., by perturbing (increasing or decreasing) the parameters ( $\theta_r$ ,  $\theta_s$ ,  $\alpha$ ,  $n$  and  $k_s$ ) by 10% one at a time in all soil layers while all other parameters are unchanged and held at the values in Table 1. The calculated recharge is compared with the recharge rate using the parameters in Table 1. The least sensitive parameter is the residual water content  $\theta_r$  with a 0.1% change in the calculated recharge, which is consistent with findings by Jimenez-Martinez et al. (2009) and Lu et al. (2011). A 10% increase in  $\theta_s$  would decrease the recharge by 7% because of larger capacity

to hold water in the soil layers. When the values of  $\alpha$  and  $k_s$  are changed by 10%, the change in recharge is no more than 4%. The most sensitive parameter is  $n$ ; increasing  $n$  by 10% result in an 8% increase in recharge.

The accuracy of field observations on precipitation, irrigation, evapotranspiration, soil water content, etc. are essential in reducing the uncertainties in recharge estimation. The uncertainty caused by water input in the CMB method has been discussed by Scanlon (2000) and Lin et al. (2013). For example, the uncertainty in the estimated recharge rates caused by chloride input could reach 35% (Scanlon, 2000). Although evapotranspiration measured by the eddy correlation method always encounters the energy closure problem (Wolf et al., 2008), fortunately, the energy balance closure of the eddy covariance systems is more than 0.94 in this study (Shen et al., 2013), which is satisfactory for analysis in this study. However, the irrigation amount could not be obtained accurately because the irrigation activity of farmers was not administered uniformly and consistently. The results of the sensitivity analysis revealed that if the irrigation amount changed by 10%, the recharge rates could change by up to 20%, indicating that the uncertainty in irrigation input would cause greater uncertainty than the model parameters. When the soil water balance method (Eq. (2)) is applied, uncertainty in other components will propagate to the recharge rates, which may cause uncertainty in recharge rates exceeding 100% (Healy and Scanlon, 2010). In arid and semi-arid areas, the recharge rate is always small relative to other water budget components, which could result in an estimated recharge rates with larger error (Scanlon et al., 2002).

## 5. Conclusions

The groundwater recharge process in the deep vadose zone (~8 m) under typical irrigated cropland in the piedmont region of the North China Plain was investigated. During the 2-year monitoring period (1 October 2011 to 30 September 2013), the gradient of total soil water potential indicated that downward water movement occurs below the root zone (2 m). The variation of the total water potential in the unsaturated zone was not obvious at a soil depths greater than 5 m at different times, indicating that a unit gradient could be applied as the lower boundary condition at these depths in vadose zone modeling. The velocity of the wetting front was approximately 0.13 m/day below the root zone, and as a result, the response time of the water table to water input might be no more than one year. Based on the in situ measurements, the average annual recharge was estimated as 223 mm/year during the monitoring period.

An unsaturated water flow model in the deep vadose zone was well calibrated using monitoring data of soil water content and matric potential. The annual recharge rates during a period of nearly four decades (from 1976 to 2013) at different depths (2–8 m, with a 1-m interval) were modeled using the calibrated model. The modeled annual recharge at a depth of 2 m ranged from 59 mm to 635 mm, with a mean value of 200 mm. The results showed that the variation in recharge flux with depth was significant on short time scales, which could contribute to different changes in soil water storage in different soil layers. The modeled average annual recharge showed fewer changes with depth (when depth > 2 m) at the 38-year scale, and the depth of 2 m below the ground surface could act as an interface for estimating the recharge at the multi-year scale.

It should be noted that the time scale during which a study was conducted could influence the representativeness of the results. For example, an estimated recharge in a study conducted during a shorter period (<12 years) might have a larger deviation (>20%) from that of a multi-year (38 years) average recharge. The variation

of annual recharge at a depth of 2 m during the period of 1976–2013 (~80%) could be explained by the water input (precipitation and irrigation) in the field. Therefore, a water input closer to the long-term annual mean or a longer study period would lead to an estimated annual recharge that was more representative of the long-term annual mean value.

We believe that the quantitative results of this work could be helpful for estimating groundwater recharge/consumption and useful for groundwater authorities and policymakers in developing more efficient strategies to manage the groundwater and ensure additional sustainability.

## Acknowledgments

This research was supported by the Natural Scientific Foundation of China (NSFC, grant no. 41471027). The authors gratefully acknowledge Dr. Qian Wang and Dr. Yucui Zhang for their participation in fieldwork.

## References

- Allen, R.G., Pereira, L.S., Raes, D., Smith, M., 1998. Crop evapotranspiration. Guidelines for computing crop water requirements. FAO Irrigation and drainage. Paper No. 56. FAO, Rome, Italy.
- Amiaz, Y., Sorek, S., Enzel, Y., Dahan, O., 2011. Solute transport in the vadose zone and groundwater during flash floods. *Water Resour. Res.* 47, W10513.
- Beven, K., Germann, P., 2013. Macropores and water flow in soils revisited. *Water Resour. Res.* 49 (6), 3071–3092.
- Carrera-Hernandez, J.J., Smerdon, B.D., Mendoza, C.A., 2012. Estimating groundwater recharge through unsaturated flow modelling: sensitivity to boundary conditions and vertical discretization. *J. Hydrol.* 452, 90–101.
- Chen, J.Y., Tang, C.Y., Yu, J.J., 2006. Use of 18O, 2H and 15N to identify nitrate contamination of groundwater in a wastewater irrigated field near the city of Shijiazhuang, China. *J. Hydrol.* 326 (1–4), 367–378.
- Dahan, O., Talby, R., Yechieli, Y., Adar, E., Lazarovitch, N., Enzel, Y., 2009. In situ monitoring of water percolation and solute transport using a vadose zone monitoring system. *Vadose Zone J.* 8 (4), 916–925.
- de Vries, J.J., Simmers, I., 2002. Groundwater recharge: an overview of processes and challenges. *Hydrogeol. J.* 10 (1), 5–17.
- Feddes, R.A., Kowalik, P.J., Zaradny, H., 1978. *Simulation of Field Water Use and Crop Yield*. Halsted Press, John Wiley & Sons Inc., New York, 189 pp.
- Harter, T., Onsoy, Y., Heeren, K., Denton, M., Weissmann, G., Hopmans, J., Horwath, W., 2005. Deep vadose zone hydrology demonstrates fate of nitrate in eastern San Joaquin Valley. *Calif. Agric.* 59 (2), 124–132.
- He, Y., Lin, W., Wang, G., 2013. In-situ monitoring on the soil water-heat movement of deep vadose zone by TDR100 system. *J. Jilin Univ. Earth Sci.* 43 (6), 1972–1979 (in Chinese with English abstract).
- Healy, R.W., Scanlon, B.R., 2010. *Estimating Groundwater Recharge*. Cambridge University Press, Cambridge, 245 pp.
- Hillel, D., 1998. *Environmental Soil Physics*. Academic Press, San Diego, 771 pp.
- Hubbell, J.M., Nicholl, M.J., Sisson, J.B., McElroy, D.L., 2004. Application of a Darcian approach to estimate liquid flux in a deep vadose zone. *Vadose Zone J.* 3 (2), 560–569.
- Jimenez-Martinez, J., Skaggs, T.H., van Genuchten, M.T., Candela, L., 2009. A root zone modelling approach to estimating groundwater recharge from irrigated areas. *J. Hydrol.* 367 (1–2), 138–149.
- Jimenez-Martinez, J., Candela, L., Molinero, J., Tamoh, K., 2010. Groundwater recharge in irrigated semi-arid areas: quantitative hydrological modelling and sensitivity analysis. *Hydrogeol. J.* 18 (8), 1811–1824.
- Kendy, E., Gerard-Marchant, P., Walter, M.T., Zhang, Y.Q., Liu, C.M., Steenhuis, T.S., 2003. A soil-water-balance approach to quantify groundwater recharge from irrigated cropland in the North China Plain. *Hydrol. Process.* 17 (10), 2011–2031.
- Kendy, E., Zhang, Y.Q., Liu, C.M., Wang, J.X., Steenhuis, T., 2004. Groundwater recharge from irrigated cropland in the North China Plain: case study of Luancheng County, Hebei Province, 1949–2000. *Hydrol. Process.* 18 (12), 2289–2302.
- Kurtzman, D., Scanlon, B.R., 2011. Groundwater recharge through vertisols: irrigated cropland vs. natural land, Israel. *Vadose Zone J.* 10 (2), 662–674.
- Leterme, B., Mallants, D., 2012. Climate and land-use change impacts on groundwater recharge. In: Oswald, S.E., Kolditz, O., Attinger, S. (Eds.), *Models – Repositories of Knowledge*. IAHS Publication, pp. 313–319.
- Lin, D., Jin, M.G., Liang, X., Zhan, H.B., 2013. Estimating groundwater recharge beneath irrigated farmland using environmental tracers fluoride, chloride and sulfate. *Hydrogeol. J.* 21 (7), 1469–1480.
- Liu, C.M., Wang, H.X., 1999. *The interface processes of water movement in the soil-crop-atmosphere system and water-saving regulations*. Science Press, Beijing, 194 pp.
- Lu, X.H., Jin, M.G., van Genuchten, M.T., Wang, B.G., 2011. Groundwater recharge at five representative sites in the Hebei Plain, China. *Ground Water* 49 (2), 286–294.

- Ma, Y., Feng, S.Y., Huo, Z.L., Song, X.F., 2011. Application of the SWAP model to simulate the field water cycle under deficit irrigation in Beijing, China. *Math. Comput. Model.* 54 (3–4), 1044–1052.
- Mualem, Y., 1976. A new model predicting the hydraulic conductivity of unsaturated porous media. *Water Resour. Res.* 12, 513–522.
- Qiu, J.T., 1992a. Moisture transport by piston-type flow in the piedmont plain zone. *Hydrogeol. Eng. Geol.* 19 (1), 30–32 (in Chinese with English abstract).
- Qiu, J.T., 1992b. Experimental study on the infiltration recharge in the region with deep water table. *Water Resour. Hydropower Eng.* 13 (5), 49–53 (in Chinese with English abstract).
- Radford, B.J., Silburn, D.M., Forster, B.A., 2009. Soil chloride and deep drainage responses to land clearing for cropping at seven sites in central Queensland, northern Australia. *J. Hydrol.* 379 (1–2), 20–29.
- Rimon, Y., Dahan, O., Nativ, R., Geyer, S., 2007. Water percolation through the deep vadose zone and groundwater recharge: preliminary results based on a new vadose zone monitoring system. *Water Resour. Res.* 43, W05402.
- Rimon, Y., Nativ, R., Dahan, O., 2011. Physical and chemical evidence for pore-scale dual-domain flow in the vadose zone. *Vadose Zone J.* 10 (1), 322–331.
- Rushton, K., 1988. Numerical and conceptual models for recharge estimation in arid and semi-arid zones. *Estimation of Natural Groundwater Recharge*. Springer, pp. 223–238.
- Scanlon, B., Healy, R., Cook, P., 2002. Choosing appropriate techniques for quantifying groundwater recharge. *Hydrogeol. J.* 10 (1), 18–39.
- Scanlon, B.R., 2000. Uncertainties in estimating water fluxes and residence times using environmental tracers in an arid unsaturated zone. *Water Resour. Res.* 36 (2), 395–409.
- Scanlon, B.R., Reedy, R.C., Gates, J.B., 2010. Effects of irrigated agroecosystems: 1. Quantity of soil water and groundwater in the southern High Plains, Texas. *Water Resour. Res.* 46 (9), W09537.
- Scanlon, B.R., Reedy, R.C., Tachovsky, J.A., 2007. Semiarid unsaturated zone chloride profiles: archives of past land use change impacts on water resources in the southern High Plains, United States. *Water Resour. Res.* 43 (6), W06423.
- Shen, Y.J., Kondoh, A., Tang, C.Y., Zhang, Y.Q., Chen, J.Y., Li, W.Q., Sakura, Y., Liu, C.M., Tanaka, T., Shimada, J., 2002. Measurement and analysis of evapotranspiration and surface conductance of a wheat canopy. *Hydrol. Process.* 16 (11), 2173–2187.
- Shen, Y.J., Zhang, Y.C., Scanlon, B.R., Lei, H.M., Yang, D.W., Yang, F., 2013. Energy/water budgets and productivity of the typical croplands irrigated with groundwater and surface water in the North China Plain. *Agric. For. Meteorol.* 181, 133–142.
- Šimůnek, J., Hopmans, J.W., 2002. Parameter optimization and nonlinear fitting. In: Dane, J.H., Topp, G.C. (Eds.), *Methods of soil analysis. Part 4 – Physical methods*. SSSA Book Series: 5. Soil Science Society of America Inc., Madison, 1692 pp.
- Šimůnek, J., Šejna, M., Saito, H., Sakai, M., van Genuchten, M.T., 2013. The HYDRUS-1D software package for simulating the one-dimensional movement of water, heat, and multiple solutes in variably-saturated media, Version 4.17. Department of Environmental Sciences, University of California Riverside, Riverside, California, USA, 307 pp.
- Sun, H., Shen, Y., Yu, Q., Flerchinger, G.N., Zhang, Y., Liu, C., Zhang, X., 2010. Effect of precipitation change on water balance and WUE of the winter wheat-summer maize rotation in the North China Plain. *Agric. Water Manage.* 97 (8), 1139–1145.
- Tan, X.C., Wu, J.W., Cai, S.Y., Yang, J.Z., 2014. Characteristics of groundwater recharge on the North China Plain. *Ground Water* 52 (5), 798–807.
- Timms, W.A., Young, R.R., Huth, N., 2012. Implications of deep drainage through saline clay for groundwater recharge and sustainable cropping in a semi-arid catchment, Australia. *Hydrol. Earth Syst. Sci.* 16 (4), 1203–1219.
- Turkeltaub, T., Dahan, O., Kurtzman, D., 2014. Investigation of groundwater recharge under agricultural fields using transient deep vadose zone data. *Vadose Zone J.* 13. <http://dx.doi.org/10.2136/vzj2013.10.0176>.
- Turkeltaub, T., Kurtzman, D., Bel, G., Dahan, O., 2015. Examination of groundwater recharge with a calibrated/validated flow model of the deep vadose zone. *J. Hydrol.* 522, 618–627.
- van Genuchten, M.T., 1980. A closed-form equation for predicting the hydraulic conductivity of unsaturated soils. *Soil Sci. Soc. Am. J.* 44, 892–898.
- von Rohden, C., Kreuzer, A., Chen, Z.Y., Kipfer, R., Aeschbach-Hertig, W., 2010. Characterizing the recharge regime of the strongly exploited aquifers of the North China Plain by environmental tracers. *Water Resour. Res.* 46, W05511.
- Wang, B.G., Jin, M.G., Nimmo, J.R., Yang, L., Wang, W.F., 2008. Estimating groundwater recharge in Hebei Plain, China under varying land use practices using tritium and bromide tracers. *J. Hydrol.* 356 (1), 209–222.
- Wesseling, J.G., Elbers, J.A., Kabat, P., van den Broek, B.J., 1991. SWATRE: instructions for input, Internal Note, Winand Staring Centre, Wageningen, the Netherlands.
- West, L.J., Truss, S.W., 2006. Borehole time domain reflectometry in layered sandstone: impact of measurement technique on vadose zone process identification. *J. Hydrol.* 319 (1–4), 143–162.
- Wohling, D.L., Leaney, F.W., Crosbie, R.S., 2012. Deep drainage estimates using multiple linear regression with percent clay content and rainfall. *Hydrol. Earth Syst. Sci.* 16 (2), 563–572.
- Wolf, A., Saliendra, N., Akshalov, K., Johnson, D.A., Laca, E., 2008. Effects of different eddy covariance correction schemes on a energy balance closure and comparisons with the modified Bowen ratio system. *Agric. Forest Meteorol.* 148 (6–7), 942–952.
- Wu, Q.H., 2013. *Quantifying Preferential Flow for the Soil Water Infiltration*. PhD Thesis, Chinese Academy of Geological Sciences, Beijing, 118 pp (in Chinese with English abstract).
- Xue, Y.Z., Gao, Y.T., 1987. Experimental study on the infiltration recharge in the region with deep water table. *Water Resour. Hydropower Eng.* 8 (11), 35–39 (in Chinese with English abstract).
- Yuan, Z.J., Shen, Y.J., 2013. Estimation of Agricultural water consumption from meteorological and yield data: a case study of Hebei, North China. *Plos One* 8 (e58685).
- Zhang, X.Y., Pei, D., Chen, S.Y., 2004. Root growth and soil water utilization of winter wheat in the North China Plain. *Hydrol. Process.* 18 (12), 2275–2287.
- Zhang, X.Y., Pei, D., Hu, C.S., 2003. Conserving groundwater for irrigation in the North China Plain. *Irrigat. Sci.* 21 (4), 159–166.
- Zhang, Y., Shen, Y., Sun, H., Gates, J.B., 2011. Evapotranspiration and its partitioning in an irrigated winter wheat field: a combined isotopic and micrometeorologic approach. *J. Hydrol.* 408 (3–4), 203–211.
- Zhang, Z.J., Fei, Y.H., 2009. *Atlas of groundwater sustainable utilization in North China Plain*. Sinomap Press, Beijing, 185 pp (in Chinese with English abstract).
- Zimmermann, U., Munnich, K.O., Roether, W., Kreutz, W., Schubach, K., Siegel, O., 1966. Tracers determine movement of soil moisture and evapotranspiration. *Science* 152 (3720), 346–347.